Fibers and Polymers (2026) 27:379–396
https://doi.org/10.1007/s12221-025-01187-6

Online ISSN 1875-0052
Print ISSN 1229-9197

REGULAR ARTICLE

Manufacturing and Structural Testing of Small Wind Turbine Blades Using Thermoplastic Composites

Rafael Carnicero[1] · Luis Cano[1] · Ignacio Cruz[1] · Juan A. García-Manrique[2]

Received: 20 May 2025 / Revised: 23 September 2025 / Accepted: 24 September 2025 / Published online: 22 October 2025

Abstract

Thermoplastic composites can be a solution for the circular economy of the wind industry. Some studies have focused on addressing the challenges of reusing raw materials and reducing both the economic costs and environmental damage. Thermoset composites have been crucial in increasing the size of wind turbines (WT), achieving longer and structurally more resistant blades, but they are difficult to recycle at the end of life and sometimes end up in landfills. Thermoplastic composites are being tested as an alternative to thermoset composites because of their similar structural properties and substantial advantages, such as ease of recycling. This article presents the results of the structural properties of a 2-m-long thermoplastic WT blade manufactured with a new thermoplastic resin called Akelite to obtain progress in the implementation of thermoplastic composites in this type of product. The new blade has been compared to an epoxy WT blade built with the same procedure. Property, static, and fatigue tests were performed on these blades to characterize them. The results of this comparison were quite similar, with less than 5% displacement in the static tests and a sensitivity change of less than 2% after the fatigue tests. Future studies should be conducted to extend this study to larger-scale blades.

Keywords Thermoplastic composite · Thermoplastic resin · Wind turbine blade · Testing · Structural properties

1 Introduction

Over the past few decades, wind turbine blades have predominantly been manufactured using thermoset composites based on epoxy or vinyl ester resins combined with E-glass fibers. While these materials have enabled substantial advancements in blade size and performance, at the end of their life (EOL), these materials present significant challenges due to their poor recyclability. Recycling methods for thermoset blades often involve high-energy processes, such as pyrolysis or mechanical shredding, which compromise fiber integrity and are economically and environmentally unsustainable. Consequently, many blades are not recycled and end up in landfills. While most WT components can be efficiently recycled [1–3], blades remain the most problematic due to their complex composite architecture based on thermoset matrices.

To overcome these limitations, this study explores using thermoplastic resin as an alternative to conventional thermosets in wind turbine (WT) blade manufacturing. Thermoplastic composites offer several advantages: they can be reheated and reshaped, and most importantly, they can be recycled by solvent dissolution, which supports a closed-loop lifecycle. In addition to being recyclable, thermoplastic resins offer manufacturing benefits such as reduced cycle time, enabling higher production throughput, and the potential for blade components to be fusion bonded without the use of adhesives. These features make thermoplastics promising candidates for next-generation WT blades. This study demonstrates the feasibility of using a novel thermoplastic resin to fabricate small-scale wind turbine blades, as tested according to the IEC 61400-23 standard [4].

✉ Rafael Carnicero
rafael.carnicero@ciemat.es

Luis Cano
luis.cano@ciemat.es

Ignacio Cruz
ignacio.cruz@ciemat.es

Juan A. García-Manrique
jugarcia@upv.edu.es

[1] Centro de Desarrollo de Energías Renovables (CEDER), CIEMAT, 42290 Soria, Spain

[2] Design and Manufacturing Research Institute, Universitat Politècnica de València, Camino de Vera, s/n, 46022 València, València, Spain

Despite the limited research in this area, promising results have been reported. For example, the ZEBRA project used Elium® thermoplastic resin to produce a 62-m blade [5]. On a smaller scale, a 1-m blade was manufactured using another thermoplastic resin (Akelite) [6], yielding comparable or improved flexural modulus and interlaminar shear strength compared to thermoset blades [7]. However, the flexural strength was found to be slightly lower. Other developments include designing segmented thermoplastic blades for large-scale applications [8], which facilitate factory manufacturing, field transport, and on-site assembly via heat welding. Several studies have investigated the fatigue behavior [9], impact resistance [10], and overall structural performance [11, 12] of thermoplastics at the component and coupon scale, confirming their viability for wind energy applications. Murray et al. [13] also validated the mechanical suitability of thermoplastics in WT blade components, emphasizing their recyclability and energy-saving potential over thermosets.

This study aims to validate the use of thermoplastic composites further by replacing the thermoset resin with Akelite [14], a novel acrylic thermoplastic developed by Institute of Polymer Science and Technology of the Spanish National Research Council (ICTP-CSIC) [15], in 2-m-long wind turbine (WT) blades. Both the thermoplastic and the reference thermoset blades were manufactured using the same fiber layout via vacuum-assisted resin (VARI) to ensure comparability. The experimental campaign includes static and fatigue testing in accordance with IEC 61400-23, to evaluate the structural integrity, service life, and performance of the blades.

Van Rijswijk et al. [16] at the Technical University of Delft pioneered in thermoplastic blade research, demonstrating that anionic polyamide-6 (PA6) could be infused via vacuum, reheated, and reshaped. Forcier and Joncas [17] developed a structural optimization framework for thermoplastic blades, demonstrating competitive fatigue and buckling performance under realistic conditions. Cousins et al. [18] performed a detailed Life Cycle Assessment (LCA) which highlighted the energy savings and GreenHouse Gas (GHG) reductions associated with the use of thermoplastics. More recently, Cheng et al. [19] presented a comprehensive review of thermoplastic materials for wind energy, encompassing processability via VARI, Automated Fiber Placement (AFP), and filament winding, in addition to thermomechanical performance and recycling strategies. Hao et al. ([20]) proposed a mild chemical recycling route to recover fiber and matrix from decommissioned blades, yielding recycled composites with enhanced interfacial adhesion and strength. Zivkovic [21] demonstrated the viability of small-scale thermoplastic blades for distributed energy systems using low-cost vacuum-assisted manufacturing techniques.

A comparative study of a 13 mm Elium® thermoplastic resin blade and a similar thermoset blade was conducted by Murray et al. [22]. The results indicated that thermoplastic resin is a viable alternative to replace thermoset resin during blade fabrication. The thermoplastic blade exhibited higher structural properties in such cases, assisting designs with reduced loads. On the other hand, using thermoplastic resin provides an additional advantage in that these composites can be restored through fusion bonding and thermoforming, as evidenced by Leon et al. [23, 24]. The final point herein proposed would simplify the maintenance of WT blades, thereby reducing costs and enhancing safety. It can thus be concluded that the utilization of thermoplastic resin in the manufacture of WT blades has the potential to engender several advantages, including reducing production costs, facilitating maintenance, and enhancing the sustainability of the recycling process. The present paper presents the findings of structural tests conducted on two diminutive wind blades. One of these has been fabricated using a novel thermoplastic resin, Akelite [14], which was developed and patented by ICTP-CSIC. The other is composed of a commercial thermoset resin. The objective of the present article is twofold: first, to provide a comparison between the two materials, and second, to achieve a significant advancement in utilizing thermoplastic resins in manufacturing small WT blades. Fatigue tests were carried out to validate the resistance of the thermoplastic blade over its anticipated 20–25 years of service life.

The collective findings from the existing literature suggest that thermoplastic composites could match or surpass the mechanical performance of thermosets in different loading and environmental conditions. It is important to note that they offer the following:

- Higher fracture toughness and damage tolerance due to ductile matrix behavior.
- Comparable fatigue life when optimized fiber architectures are employed.
- Stable performance under thermal cycling, critical for offshore and alpine environments.

Additionally, thermoplastics allow for fusion bonding, making them ideal for modular, segmented blade designs and enabling the transportation and assembly of long blades. From a sustainability standpoint, thermoplastics offer a transformative advantage. Unlike thermosets, which require destructive, energy-intensive recycling methods, thermoplastics can be melted or dissolved for reuse. Recent studies [19, 20] have confirmed the feasibility of solvent-based recycling, thereby aligning with the principles of the circular economy.

Thermoplastic composites have some advantages compared with thermoset composites such as higher production rate due to its reduced cycle time; also, small superficial delamination are reparable by thermal application. In addition, thermoplastic composites are easily recyclable by chemical process such as dissolution into a solvent. Actually, Akelite resin costs are a bit higher comparing with the commercial epoxy resin, but extrapolating for large-scale production would obtain similar costs. Nowadays, a life cycle assessment (LCA) and a life cost costing (LCC) are being developing to evaluate the influence of the Akelite thermoplastic resin for large-scale production.

Life cycle assessments indicate that the production of thermoplastic blades can have the following consequences:

- Up to 40% reduction in GHG emissions.
- Approximately 20% lower energy consumption over the blade's life cycle.
- The reuse of fibers and matrices has led to a 50% reduction in waste generation at EOL.

Nevertheless, key challenges must be addressed:

1. **Scaling up** from small-scale prototypes to full-size blade demonstrations.
2. **Processing constraints** involving high temperature and pressure requirements.
3. **Lack of standardization** for design, testing, and certification procedures.
4. **Integration of structural and functional systems** (e.g., sensors, lightning protection).

2 Materials and Methods

2.1 Blade Design

A 2-m-long wind turbine blade was designed using the open-source QBlade software [25]. The blade's mechanical properties and static behavior were simulated using SolidWorks [26] and BladeFS [27], the latter of which was developed by the National Renewable Energy Laboratory (NREL).

QBlade was also employed to define the blade's external geometry and simulate its aerodynamic performance. The blade profile was based on the SG6043 airfoil developed by Selig and Giguère (SG) [28]. This airfoil features a maximum thickness of 5.1%, located at 49.7% of the chord, and a relative thickness of 10.0%, positioned at 32.1% of the chord. Two additional transitional profiles derived from the SG6043 were employed to facilitate a smooth transition from the cylindrical root to the aerodynamic region. The twist angle was set to 15° at the location of the maximum chord, decreasing linearly to 0° at the blade tip. Figure 1 shows the QBlade-generated model of the 2-m blade, segmented into 80-mm sections.

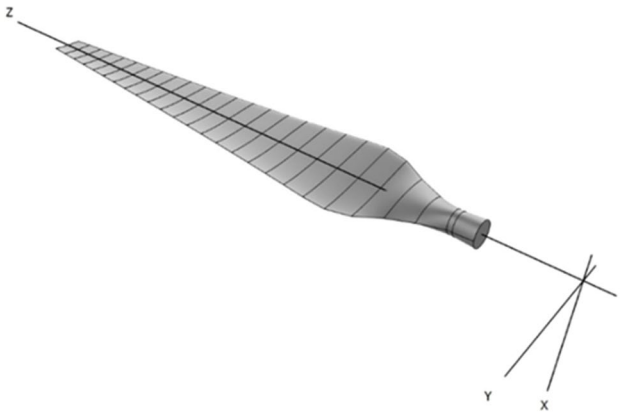

Fig. 1 Model of 2-m blade

The thermoset blade was fabricated using unidirectional fiberglass from Gavazzi Tessuti Tecnici [29] and Sicomin [30] epoxy resin. The same fiber architecture was applied to the thermoplastic blade, which used Akelite thermoplastic resin instead. All blades followed a symmetrical laminate configuration. In the root section (up to 0.67 ms from the root), the stacking sequence included 13 layers in the order [±45 G/0 G/±45 G/0 G/90 G/0 G/90 G], yielding a total thickness of 5 mms. In the middle section (from 0.67 m to 1.33 m span), nine layers were applied in the sequence [±45 G/0 G/±45 G/0 G/90 G], resulting in a thickness of 3.76 mm. Finally, the tip section (from 1.33 m to the blade tip) incorporated five layers in the sequence [±45 G/0 G/90 G], yielding a thickness of 2 mm.

2.2 Mold Manufacturing

The mold design process began in SolidWorks, using the blade geometry previously defined in QBlade. Each half-mold was divided into two sections, yielding a total of four parts. This segmentation was necessary to accommodate the print volume limitations of the available 3D printer [31] and to optimize the build orientation, reducing warping and improving dimensional stability during the printing process. Figure 2 illustrates one of these half-molds, already split into two parts and prepared for printing. For the manufacturing of the mold parts, a hybrid process combining Fused Filament Fabrication (FFF) and CNC machining was employed. The initial geometry was 3D printed using LNP^{TM} THERMOCOMP^{TM} AC004XXAR1 [32], an ABS-based thermoplastic resin reinforced with 20% carbon fiber. This composite material was selected for its excellent mechanical stiffness, thermal resistance, and low thermal expansion, all of which are critical for maintaining dimensional stability during resin infusion and curing.

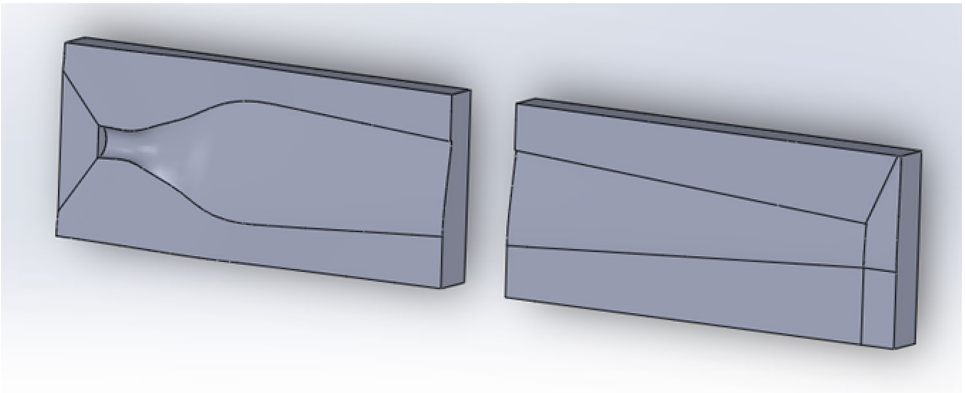

Fig. 2 Design of half-mold cut into two parts for 3D printing

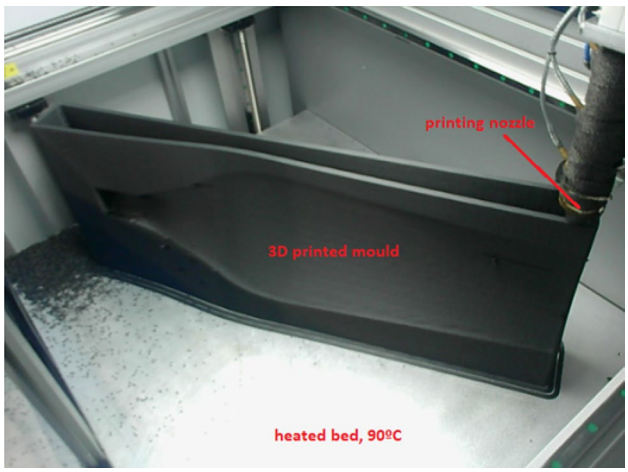

Fig. 3 3D printing of a part of the mold

The 3D printing process was performed in layers of approximately 0.4 mm, with a high infill density to ensure the mechanical rigidity of the mold under vacuum pressure during the VARI process. The total print time for each part ranged from 20 to 35 h, depending on geometry and build height. Figure 3 shows the 3D printing process in progress for one of the mold sections. In this figure, the layered structure of the printed material is clearly visible, and the infill pattern used to reinforce the structure can also be observed. The part is being printed vertically on a heated bed to minimize warping. Once all four parts were printed, they were mechanically joined using precision alignment features designed into the CAD model. The 3D printing process was oversized 2 mm bigger, to have a rough finish. Later, it was corrected with a milling of the mold using a CNC machine, obtaining a fine finish within tolerances.

After assembly, CNC machining was performed on the key surfaces of the complete mold to improve dimensional accuracy, particularly in the contact zones between the mold halves and at the blade surface interface. This step ensured tight tolerances and perfect alignment during blade layup. Finally, the mold was polished manually using fine-grit abrasives and polishing compounds. This surface finishing step was critical to obtain a smooth internal surface, which directly affects the quality of the composite blade skin and ensures easy demolding after curing. Proper surface finish also helps reduce resin pooling and eliminates surface defects in the blade.

2.3 Blade Manufacturing

The manufacturing of both epoxy and thermoplastic blades was carried out using the same mold, previously described in Sect. 2.2, and employed a VARI process. Akelite thermoplastic resin has been developed to be used in the same way as commercial thermosetting resins in the infusion of large composite parts such as wind turbine blades. Parameters such as resin density or viscosity have been adjusted to obtain a thermoplastic resin capable of being used in VARI processes. Reference [14] is the patent for the Akelite resin, which has been used in this research to show the feasibility of replacing current thermosetting resins with thermoplastic resin in the manufacture of large and complex parts using composite materials. The use of the same production process ensured consistent manufacturing conditions, allowing direct comparison between the blades. The process began with the placement of dry fiber reinforcements in the mold. Both blades used identical laminate stacking sequences, as outlined in Sect. 2.1, and employed unidirectional and biaxial glass fiber fabrics from Gavazzi Tessuti Tecnici [29]. These were arranged over the internal mold surface according to the defined blade geometry, with particular attention to fiber orientation and alignment to preserve structural symmetry and reproducibility.

A peel ply layer was applied over the reinforcement to facilitate demolding and ensure a clean surface for subsequent bonding. A flow media was then placed to enhance resin distribution, followed by resin inlet channels and vacuum outlet lines. The resin inlet was positioned centrally on the blade mold to promote symmetric infusion,

while two vacuum ports were located at the extremes to draw the resin longitudinally through the laminate. Figure 4 illustrates the setup during the infusion of a thermoplastic blade half.

The infusion process was carried out under ambient temperature (23°C). A vacuum of -0.8×10^5 Pa was applied using a vacuum pump connected to both ends of the mold, while a positive pressure of 0.95×10^5 Pa was maintained in the resin inlet line. This pressure differential enabled uniform resin flow throughout the fiber preform. Both the epoxy and thermoplastic resins had a similar viscosity of approximately 1100 mPa· s, allowing comparable flow characteristics. The epoxy system used was Sicomin SR-1280 resin with SD-4772 hardener, mixed at a weight ratio of 100:27. In contrast, the thermoplastic blade was infused with Akelite resin, an acrylic-based system consisting of Part A (base resin) and Part B (benzoyl peroxide initiator) mixed at a weight ratio of 97:3. Table 1 summarizes the properties of both resin systems.

After complete infusion, the curing conditions differed between the two blade types:

- **Epoxy blade**: Cured at room temperature (23°C) for 24 h, followed by a post-curing stage at 60°C for 16 h to enhance mechanical properties and dimensional stability.
- **Thermoplastic blade**: Polymerized at 70°C for 2 h, during which a notable exothermic reaction was observed, indicating rapid thermoplastic chain formation and solidification.

Once both halves of each blade had been cured and demoulded, the two halves were bonded together using a two-component epoxy adhesive (Sicomin Isobond 735 [33]), which was mixed at a weight ratio of 100:50. Moderate pressure was applied during the bonding process to ensure tight contact and adhesive spread throughout the joint interface. To ensure experimental consistency, the entire manufacturing process was replicated twice—once for the epoxy blade and once for the thermoplastic blade—under identical environmental and process conditions. Each blade underwent visual inspection to assess surface finish, uniformity, and potential defects such as dry spots or resin-rich zones. This rigorous control over materials, process parameters, and layup configuration ensured that the only variable between the two manufactured blades was the resin system.

2.4 Blade Testing

This section describes the tests that were conducted to determine the structural properties of the blades. Property, and static and fatigue tests were conducted to characterize the blades structurally. The total sequence of these tests were: (1) Property test, (2) Static test, (3) Fatigue test, (4) Post-fatigue static test, and (5) Final property test. Table 2 lists

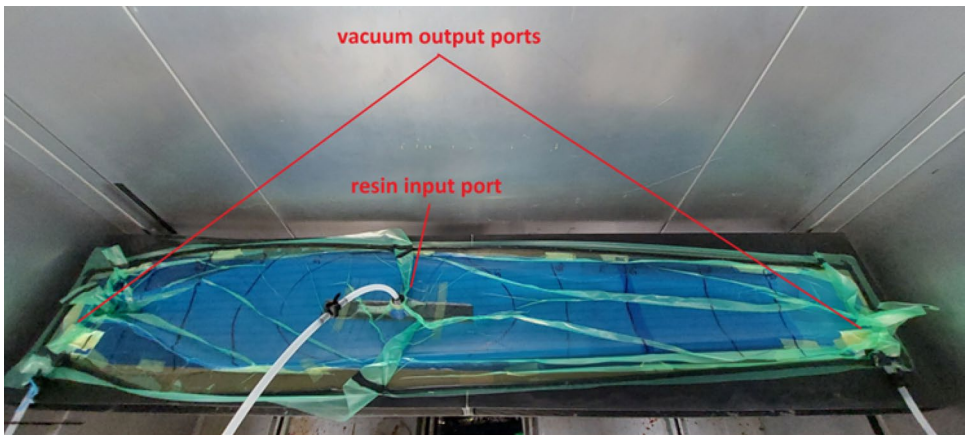

Fig. 4 Infusion process of a thermoplastic blade half using the VARI technique

Table 1 Properties of materials used in the epoxy and thermoplastic blades

Trade name	Description	Density	Mix ratio	Blade
Gavazzi Tessuti - 8092	Unidirectional fiberglass	625 g/m^2	N/A	Both
Gavazzi Tessuti - BXE600	Biaxial fiberglass	600 g/m^2	N/A	Both
Sicomin SR-1280	Epoxy resin	1153 kg/m^3	100	Epoxy
Sicomin SD-4772	Hardener	944 kg/m^3	27	Epoxy
Akelite (Part A)	Acrylic thermoplastic resin	1180 kg/m^3	0.97	Thermoplas
Akelite (Part B)	Benzoyl peroxide initiator	1150 kg/m^3	0.03	Thermoplas
Sicomin Isobond 735	Bonding adhesive	1240 kg/m^3	100:50	Both

Table 2 Equipment used for testing

Instrument	Manufacturer	Model	Uncertainty	Testing
Accelerometer	PCB Piezotronics	352C33	3.0%	Property
Calibrator of accel	Brüel & Jaer	4294	0.1%	Property
Weight scale	Kern	FCB 24k2	0.1%	Property
Tape measure	Hultafors	TK8M	0.3%	Property
Temperature	Comet	T0210	1.0°C	Static
Humidity	Comet	T0210	3.0%	Static
Load Cell	Bongshin	DBBP-0.5t	0.3%	Static
String Pot	ASM	WS17KT-1500	0.2%	Static / Fatigue
Strain Gage	HBM	K-LY41-350	–	Static / Fatigue

the equipment used for the different tests, along with the uncertainty estimates for the recorded measurements at a 95% confidence level (k=2). The loads applied in the static and fatigue tests were estimated using the equations of the simplified load model (SLM) described in the IEC 61400-2 standard [34] and the book [35]. The small WT design for this study was a 3.5 kW turbine operating at 250 rpm in WT class III conditions (average wind speed of 7.5 m/s). In addition, the blade length was defined as 2 m.

2.4.1 Property Testing

A series of characterization tests were conducted on the blades to determine their basic physical and dynamic properties before they were subjected to mechanical loading. This included measuring the blades' mass and center of gravity (CG), as well as their natural frequencies in flapwise and edgewise directions. These procedures ensured baseline comparability between the epoxy and thermoplastic blades prior to static and fatigue testing. The mass of each blade was measured using a precision digital scale (Kern FCB 24k2) with an expanded uncertainty of 0.1% (coverage factor k = 2). To determine the center of gravity, each blade was suspended from multiple positions by a rope until static equilibrium was achieved. The intersection of vertical lines projected from these suspension points identified the center of gravity location along the blade's longitudinal axis. Measurements were taken using a calibrated tape measure (Hultafors TK8M) with an accuracy of 0.3%.

The dynamic characterization focused on identifying the first natural frequencies in both the flapwise and edgewise directions. Each blade was mounted horizontally in a cantilever configuration with the root section fixed rigidly to a test bench. An accelerometer (PCB Piezotronics 352C33, with an expanded uncertainty of 3.0%) was positioned 90% of the way along the blade from the root. A calibrated impact hammer was then used to excite vibrations at 70% of the span in the desired direction. The response signal was processed using a fast Fourier transform (FFT) to extract the dominant frequency peaks. Each test was repeated three times to verify repeatability and mitigate experimental noise. Figure 5 shows the test configuration during the modal analysis.

Fig. 5 Property test: measurement of natural frequencies

Table 3 Summary of property testing results for both blades

Characteristic	Epoxy Blade	Thermoplastic Blade	Difference (%)
Mass (g)	6798	6302	−7.3
CG from root (mm)	795	783	−1.5
1st Flapwise Frequency (Hz)	9.22	10.45	+13.3
1st Lead-Lag Frequency (Hz)	18.84	18.75	−0.5

The results of these tests are summarized in Table 3. Note that the thermoplastic blade was 7.3% lighter than the epoxy blade. Additionally, its center of gravity was 1.5% closer to the root, potentially due to localized resin mass distribution. In terms of modal behavior, both blades displayed similar

initial edgewise frequencies. However, the thermoplastic blade exhibited a 13.3% increase in the first flapwise frequency, indicating slightly higher stiffness in that direction.

2.4.2 Static Testing

The objective of the static test was to evaluate the structural response of the blades under maximum design loads, thereby simulating extreme wind conditions in accordance with the IEC 61400-23 standard [34]. The test focused on measuring tip displacement and distributed strain responses to assess stiffness and deformation behavior. The blade under test was installed in a cantilever configuration, fixed at the root with loading applied at two specific stations: 640 mm and 1440 mm from the root. These positions were selected based on the load distribution obtained through the Simplified Load Model (SLM). The loads were applied using a pair of winches connected to saddles that clamped the blade in place at these spanwise positions. Load cells (Bongshin DBBP-0.5t, expanded uncertainty 0.3%) were installed alongside the winch cables to monitor the applied forces in real time.

Three strain gauges (HBM K-LY41-350) were bonded to the blade surface at 80 mm, 480 mm, and 1000 mm positions relative to the root, on the sparcap of blade pressure side aligned at Z-axis (Fig. 6, Top). These sensors recorded localized strains during loading, enabling the computation of internal bending moments and stress distributions. Additionally, a string potentiometer (ASM WS17KT-1500, uncertainty 0.2%) was attached to the blade tip to measure vertical deflection in the flapwise direction. Ambient laboratory conditions were monitored throughout the test using a temperature and humidity sensor (Comet T0210) to ensure values remained stable within ±1.0 °C and ±3.0% relative humidity, respectively, thereby reducing environmental variability. The blade was subjected to four loading steps, each applying a force of 125 N, with the steps being applied simultaneously at loading stations 640 mm and 1440 mm apart. Each step was held for 20 s before moving on to the next. Once the maximum load of 500 N had been reached at each saddle, the load was unloaded in reverse steps to simulate the unloading phase and detect any residual deformation. During the test, the blade was loaded in four 125 N

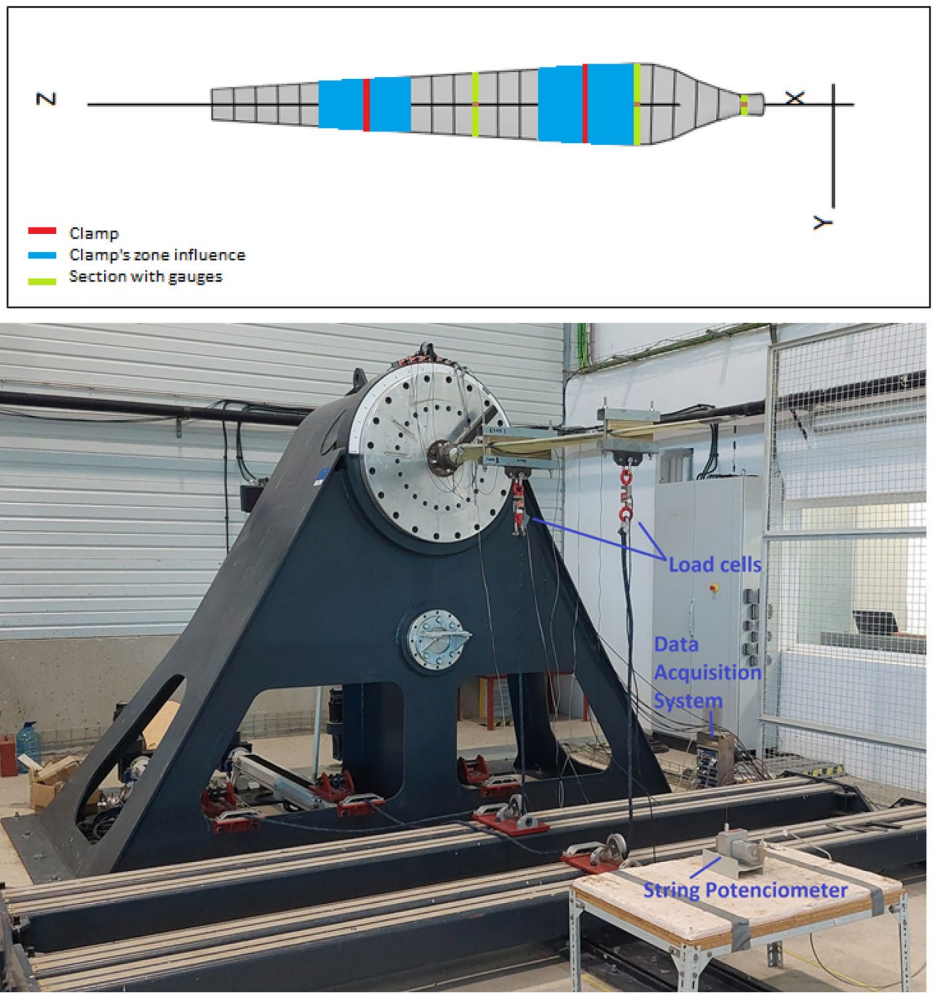

Fig. 6 Scheme of Clamp's zone influence and strain gauge positions (top). Static test configuration showing load application points and displacement measurement at blade tip (down)

steps, held for 20 s and then released proportionately. Figure 6 shows the setup of the static thermoplastic blade test.

The total bending moment at the root was approximately 1140 Nm under full loading. The blade deflection and strain responses were monitored at each load increment. Tables 4 and 5 show the summary of both initial static test performed to the epoxy and thermoplastic blades, respectively.

2.4.3 Fatigue Testing

Fatigue testing was performed to simulate the long-term operational loads expected to be experienced by wind turbine blades over their 20- to 25-year service life. The test aimed to validate the structural durability of thermoplastic and epoxy blades under repeated cyclic loading. The procedure adhered to the guidelines set out in IEC 61400-23 and employed the Damage Equivalent Load (DEL) methodology to design the fatigue loading profile.

The fatigue test was designed to reach a target of 10^6 cycles. To reduce the time taken for the test, an increased load amplitude was used while maintaining an equivalent damage profile. The applied moment for fatigue was calculated using the simplified load model (SLM), and the damage equivalent load (DEL) was computed as follows:

$$d_i = \left(\frac{M_a}{M_u}\right)^m \cdot \frac{N_a}{N_{eq}} \tag{1}$$

$$D = \sum d_i \tag{2}$$

$$\mathrm{DEL} = M_u \cdot D^{1/m}, \tag{3}$$

where

- M_a is the applied moment,
- M_u is the target moment,
- m is the inverse fatigue slope (taken as 10),
- N_a is the number of cycles at load M_a,
- N_{eq} is the reference number of cycles (1,000,000).

Table 4 Initial static test of epoxy blade

Saddle 1 [N]	Saddle 2 [N]	Root moment [Nm]	Moment 1 [Nm]	Moment 2 [Nm]	Moment 3 [Nm]	Strain 1 [μ m/m]	Strain 2 [μ m/m]	Strain 3 [μ m/m]	Tip displacement [mm]
30.00	25.00	98.50	89.77	48.87	17.45	−0.53	1.12	1.50	0.39
167.20	142.10	354.68	325.86	183.24	68.98	373.20	93.41	102.50	31.55
300.80	276.30	633.17	583.19	333.45	128.03	810.10	205.10	215.40	69.84
432.10	391.70	883.13	813.66	465.24	178.80	1174.00	310.20	311.10	106.50
546.90	536.40	1164.71	1074.74	622.52	242.47	1629.00	446.40	426.90	152.70
390.20	395.40	861.68	795.23	462.09	180.43	1145.00	313.10	317.00	115.90
298.50	261.90	610.97	562.32	319.26	121.69	750.20	196.80	206.30	82.96
165.20	149.00	363.33	334.12	189.55	72.01	333.60	99.85	110.00	47.43
34.22	25.96	102.58	93.44	50.47	17.88	−54.49	3.35	4.27	9.39

Table 5 Initial static test of thermoplastic blade

Saddle 1 [N]	Saddle 2 [N]	Root moment [Nm]	Moment 1 [Nm]	Moment 2 [Nm]	Moment 3 [Nm]	Strain 1 [μ c1m/m]	Strain 2 [μ m/m]	Strain 3 [μ m/m]	Tip displacement [mm]
30.00	25.00	98.50	89.77	48.87	17.45	−3.12	−0.21	−0.02	0.47
154.50	149.00	356.50	328.13	187.83	72.01	443.40	92.56	128.80	34.74
273.80	245.70	571.88	526.45	299.75	114.56	810.00	169.00	225.90	65.98
405.40	376.10	843.62	777.49	445.99	171.94	1065.00	238.30	352.20	169.40
474.60	442.40	983.24	906.41	520.71	201.11	1467.00	325.90	412.40	234.30
406.40	368.90	833.90	768.26	439.24	168.77	1042.00	293.50	345.30	220.10
285.60	265.10	607.34	559.44	320.27	123.10	624.20	218.10	243.50	195.40
162.90	156.50	372.66	343.04	196.38	75.31	198.30	145.30	135.30	165.60
26.14	22.94	93.07	84.81	46.28	16.55	−133.60	−8.24	−1.36	22.76

Fig. 7 Fatigue test setup for thermoplastic blade with horizontal crank and saddle load application at 1.44 m

Table 6 Strain vs load calibration results for both blades

Epoxy blade			
Station	Moment [Nm]	Range strain [μm/m]	Sensitivity [Nm/(μm/m)]
Section 1 (0.08m)	243	285.4	0.85
Section 2 (0.48m)	164	109.9	1.49
Section 3 (1.00m)	72	130.6	0.55
Thermoplastic blade			
Section 1 (0.08m)	243	369.5	0.66
Section 2 (0.48m)	164	97.8	1.68
Section 3 (1.00m)	72	143.2	0.50

The calculated target moments at three blade sections were: 440 Nm (0.08 m), 270 Nm (0.48 m), and 120 Nm (1.0 m). These values were used to control the fatigue load profile throughout the test. The blade was mounted horizontally on a custom fatigue test bench and clamped at the root. A horizontal, crank-driven actuator applied cyclic, sinusoidal loads in the flapwise direction via a saddle positioned 1.44 m from the root. The crank amplitude was adjusted to match the maximum target displacement. The test frequency was selected, so that heat generation and inertial effects would remain negligible (Fig. 7). Three strain gauges, which had previously been used in the static test at 0.08 m, 0.48 m, and 1.0 m, were used to monitor strain and moment during the fatigue test. No load cell was used during the test; instead, moment estimation was derived from the strain–moment calibration curves obtained from pre-test static loading.

Table 6 shows the summary of the sensitivity values obtained to measure indirectly the applied moment during fatigue test using the strain gauges, during the calibration static test.

Once the calibration static test was performed, the blade was cycling during 10^6 cycles. This static calibration test was repeated at three intervals: 0%, 50%, and 100% of the fatigue life. During each test, a static load of 150 N was applied, and the strain at 0.08 m, 0.48 m, and 1.0 m, and displacement of the blade tip were measured.

The damage equivalent load (DEL) was calculated using Eqs. 1, 2, 3. The applied moment M_a was obtained multiplying the strain range (Max.strain–min.strain) by the sensitivity calculated at the calibration static test. Then, damage di for each cycle was calculated. At the end of fatigue test, total damage D and damage equivalent load DEL were calculated. Figure 8 shows the first cycles of fatigue tests for epoxy and thermoplastic blades. Using the sensitivity obtained at the calibration static test, the applied moment was calculated for the three sections 0.08 m, 0.48 m, and 1.0 m.

The total cycles applied to epoxy blade was 1,036,842 cycles and that to thermoplastic blade was 1,140,795 cycles. Figure 9 shows the total cycles of fatigue tests for epoxy and thermoplastic blades.

2.4.4 Post-fatigue Static Testing

After fatigue tests, the static test was repeated to compare strains and displacements. Table 7 and Table 8 show the summary of both post-fatigue static test performed to the epoxy and thermoplastic blades, respectively.

2.4.5 Final Property Testing

The final test conducted was a property test to compare natural frequencies, center of gravity, and mass. Table 9 shows the summary of property tests performed to the epoxy and thermoplastic blades respectively.

3 Results

This section compares the results of the different tests performed on the two blades (epoxy and thermoplastic) to analyze their behavior.

3.1 Property Response Results

This section presents the results of the property tests conducted prior and after to mechanical loading. These tests provided a baseline for the physical and dynamic characteristics of the two blades, which are essential for assessing structural comparability. The thermoplastic blade had a total mass of 6302 g, while the epoxy blade weighed 6798 g. This represents a weight reduction of approximately 7.3% for the thermoplastic blade, which is attributed to the slightly lower density of the Akelite matrix and possible differences

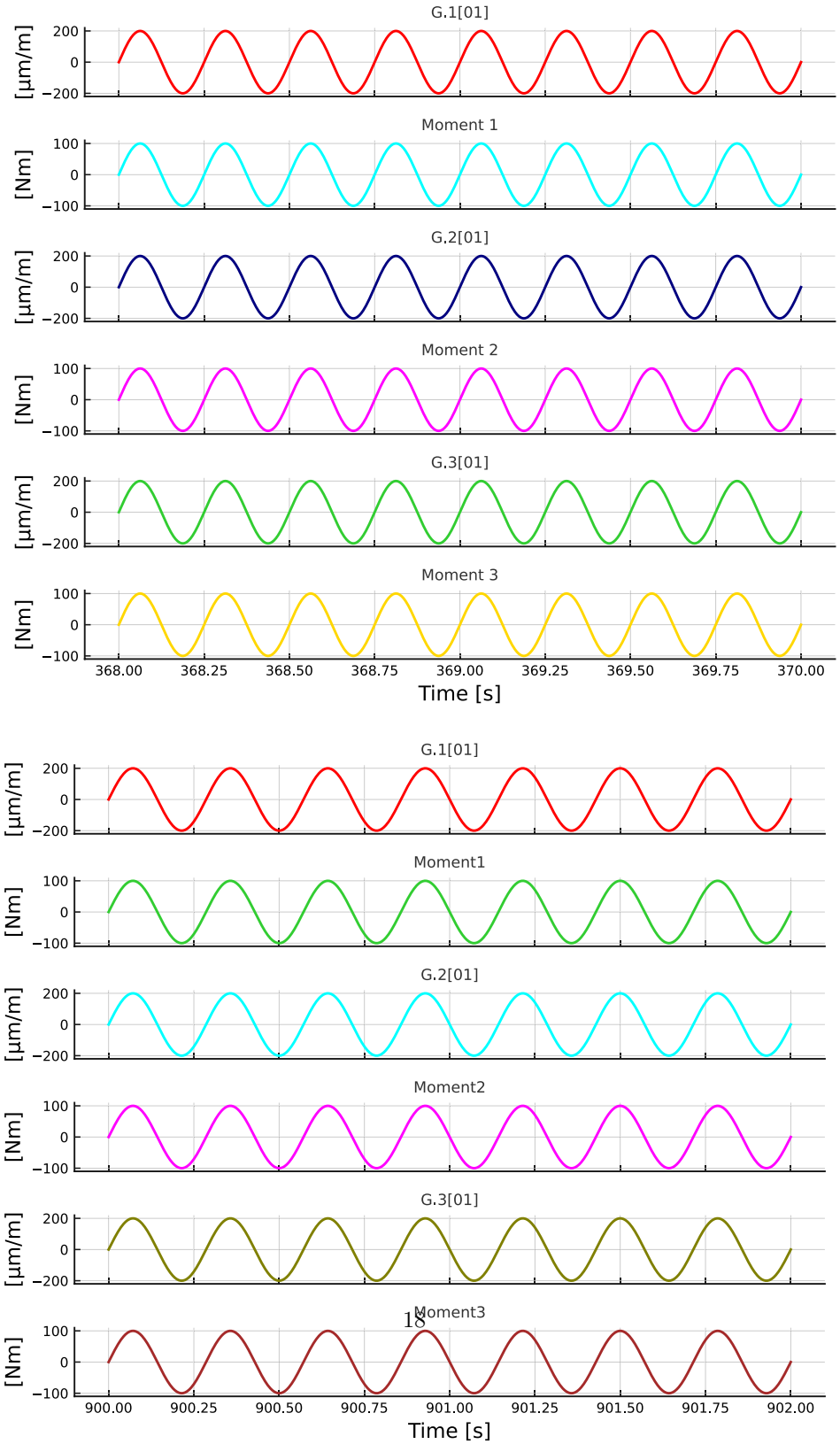

Fig. 8 Strains and corresponding bending moments at 0.08 m (G.1), 0.48 m (G.2), and 1.0 m (G.3) stations during initial fatigue cycles. Top: epoxy blade. Down: thermoplastic blade

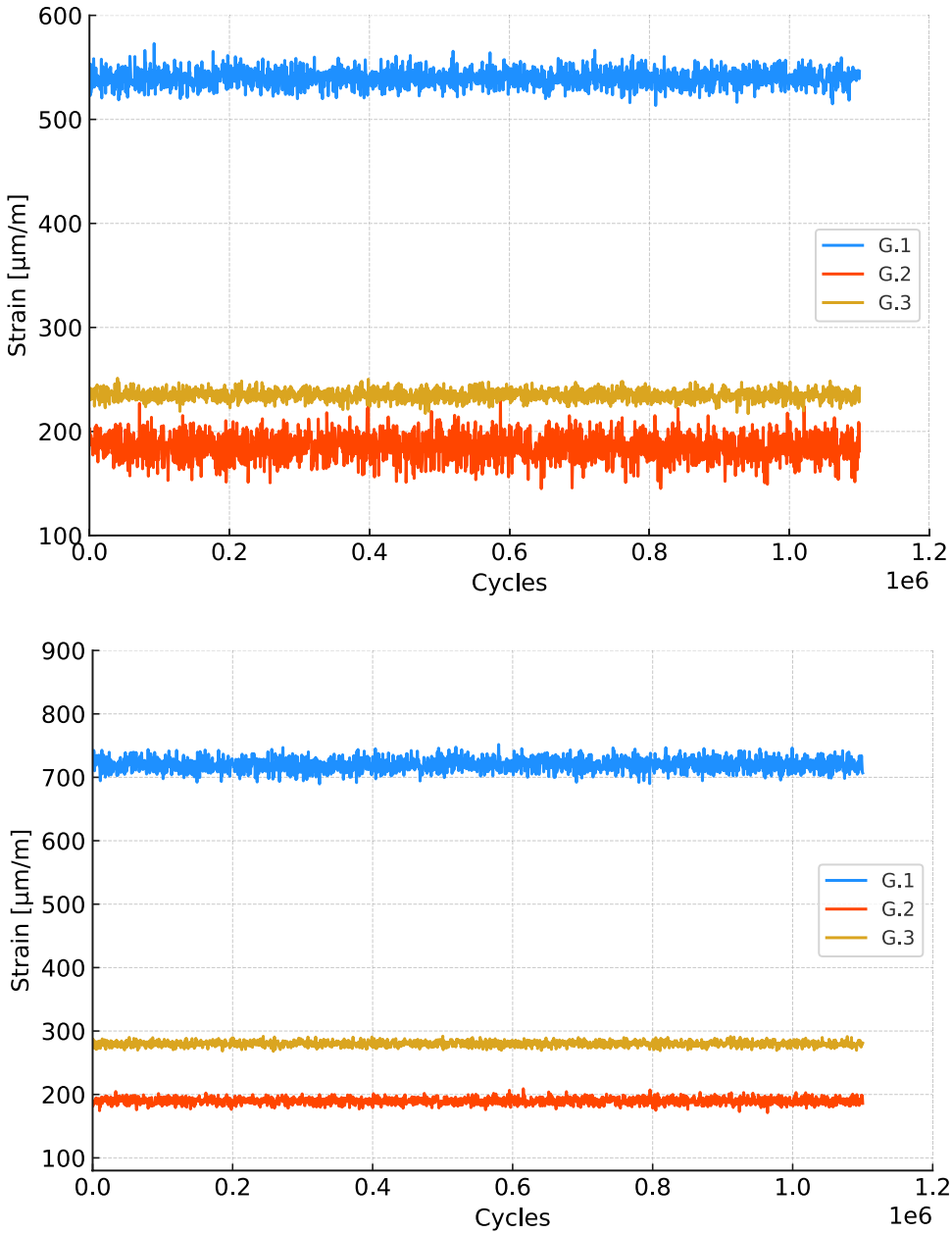

Fig. 9 Strains at 0.08 m (G.1), 0.48 m (G.2), and 1.0 m (G.3) stations of fatigue test. Top: epoxy blade. Down: thermoplastic blade

in resin absorption during infusion. Also, the manual process of bonding two shells with structural adhesive could influence to this lower weight of the thermoplastic blade.

The center of gravity (CG), measured from the blade root, was found to be 795 mm for the epoxy blade and 783 mm for the thermoplastic blade. This 1.5% difference suggests a slight redistribution of mass toward the root of the thermoplastic blade, possibly due to localized resin pooling or minor variations in fiber placement during layup. Dynamic modal testing revealed very similar behavior in the edgewise (lead–lag) direction, with the first natural frequencies being 18.84 Hz and 18.75 Hz for the epoxy and thermoplastic blades, respectively—an insignificant deviation of 0.5%.

However, a more significant difference was observed in the flapwise direction. The thermoplastic blade had a first natural frequency of 10.45 Hz, compared to 9.22 Hz for the epoxy blade, a 13.3% increase. This suggests slightly higher flexural stiffness in the flapwise direction, which could be due to improved resin–fiber interaction or reduced damping associated with the thermoplastic matrix. Figure 10 shows how the vibration of both blades decayed following manual excitation in the flapwise direction. The vibration amplitude of both blades decreased to negligible levels within approximately 5 s. The damping behavior was qualitatively similar, with no significant evidence of increased energy dissipation in either system. This confirms that using a thermoplastic

Table 7 Post-fatigue static test of epoxy blade

Saddle 1 [N]	Saddle 2 [N]	Root moment [Nm]	Moment 1 [Nm]	Moment 2 [Nm]	Moment 3 [Nm]	Strain 1 [μ m/m]	Strain 2 [μ m/m]	Strain 3 [μ m/m]	Tip displacement [mm]
30.00	25.00	98.50	89.77	48.87	17.45	4.66	1.36	1.43	0.53
170.40	149.20	366.94	337.31	190.57	72.10	378.90	107.00	110.60	35.18
272.40	278.40	618.04	570.14	330.92	128.95	775.30	213.70	223.10	78.78
394.10	399.40	869.93	802.85	466.55	182.19	1251.00	318.90	325.90	130.80
534.00	528.70	1145.38	1057.04	613.07	239.08	1767.00	442.60	432.10	187.10
397.70	402.50	876.69	809.08	470.11	183.55	1323.00	316.00	329.10	153.80
287.30	273.20	620.08	571.41	328.31	126.66	863.10	197.60	220.10	119.20
155.60	149.10	357.34	328.88	188.11	72.06	407.10	83.42	109.80	80.20
32.64	25.93	101.52	92.51	50.19	17.86	53.77	−21.04	1.43	41.71

Table 8 Post-fatigue static test of thermoplastic blade

Saddle 1 [N]	Saddle 2 [N]	Root moment [Nm]	Moment 1 [Nm]	Moment 2 [Nm]	Moment 3 [Nm]	Strain 1 [μ c1m/m]	Strain 2 [μ m/m]	Strain 3 [μ m/m]	Tip displacement [mm]
30.00	25.00	98.50	89.77	48.87	17.45	−0.10	−0.01	−0.33	0.00
156.50	153.90	364.82	335.92	192.86	74.17	437.10	95.73	125.70	32.30
276.80	284.00	628.91	580.22	337.00	131.41	877.20	192.10	249.80	78.36
407.20	397.60	875.71	807.74	466.92	181.40	1293.00	284.50	355.00	121.30
530.70	527.50	1141.55	1053.56	611.39	238.55	1862.00	394.00	471.20	178.60
406.10	400.50	879.18	811.07	469.53	182.67	1442.00	288.20	357.40	153.60
280.30	269.40	610.14	562.32	323.55	124.99	1006.00	180.00	234.10	124.90
154.30	151.10	359.39	330.88	189.82	72.94	592.10	83.55	121.30	96.09
29.61	25.36	98.77	90.04	49.15	17.61	99.35	−12.61	−0.75	47.02

Table 9 Summary of final property testing results for both blades

Characteristic	Epoxy blade	Thermoplastic blade	Difference (%)
Mass (g)	6,794	6,314	−7.1
CG from root (mm)	796	783	−1.6
1st Flapwise Frequency (Hz)	8.92	10.31	+15.6
1st Lead-Lag Frequency (Hz)	18.60	20.16	+8.4

resin does not affect the dynamic response of the blade during small-amplitude oscillations.

After all static, fatigue, and post-fatigue static tests, a final property test was carried out to compare compare the initial and final results regarding property values. The main initial property test results are summarized in Table 3. These values confirm that the two blades are dynamically and physically comparable, thus validating their suitability for subsequent structural testing. The results of the final property tests are summarized in Table 9. Mass and center of gravity were almost the same. While flapwise frequency variation was 3.3% and 1.3% for edgewise frequency of the epoxy blade; the thermoplastic blade results were a variation of 1.3% at flapwise frequency and 7.5% for edgewise frequency.

3.2 Static Response Results

This section presents the structural response of both blades under quasi-static loading conditions. The objective was to evaluate their stiffness and deformation characteristics under severe loading conditions using the Simplified Load Model (SLM) methodology outlined in IEC 61400-2. The test setup and procedure are detailed in Sect. 2.4.2. Each blade was subjected to four load increments of 125 N, applied at two stations (640 mm and 1440 mm from the root) using pulling saddles connected to winches. The total applied load resulting from this was 500 N per station, producing a combined moment at the blade root of approximately 1,140 Nm. This value corresponds to the maximum static design load

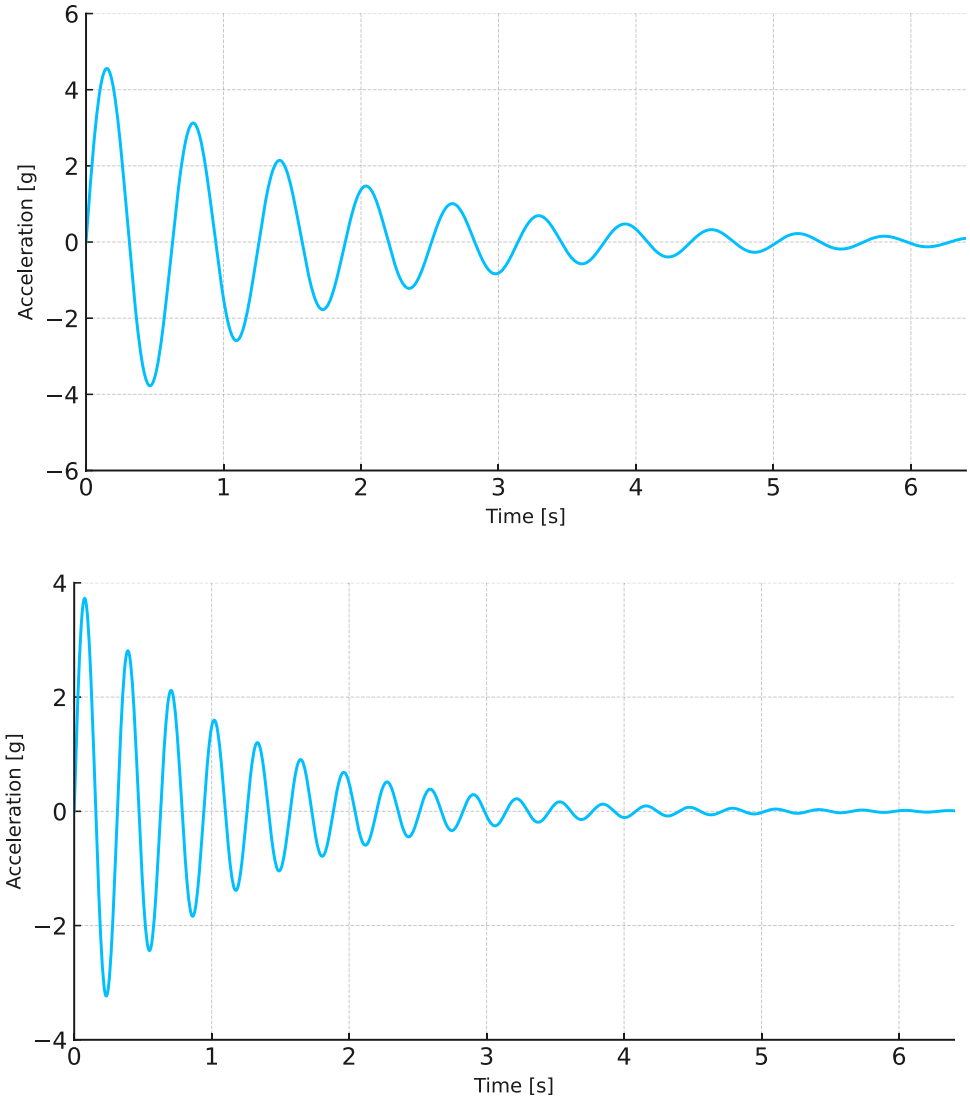

Fig. 10 Damping response. Top: epoxy blade. Down: thermoplastic blade

expected during extreme wind events in a 3.5 kW Class III small wind turbine operating at 250 rpm.

Figures 11 and 12 show the summary of the initial and post-fatigue static tests carried out on the epoxy blade. Figure 11 shows the measured epoxy blade tip displacement in the flapwise direction as a function of the applied root moment. And Fig. 12 shows the measured strain for each section moment (0.08 m, 0.48 m, and 1.0 m) for epoxy blade. A residual strength less than 5% for the three strain gauges was obtained for the epoxy blade at the end of fatigue test. An a deviation of 34 mm at maximum applied moment was obtained, it means 22.5%.

Similarly, Figs. 13 and 14 show the summary of the initial and post-fatigue static tests carried out on the thermoplastic blade. In that case, a residual strength less than 5% for the three strain gauges was obtained for the thermoplastic blade at the end of post-fatigue static test. In addition, a variation of 55 mm at maximum applied moment was obtained; it

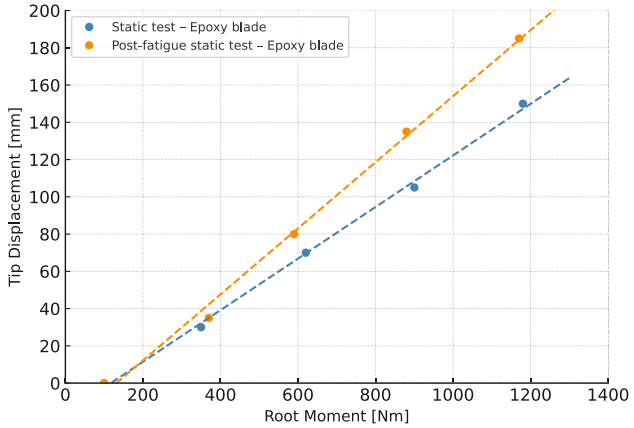

Fig. 11 Tip displacement of epoxy blade for initial and final static tests

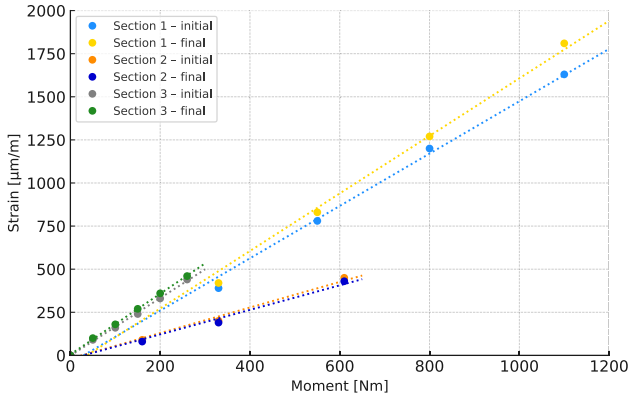

Fig. 12 Strain at different sections of epoxy blade for initial and final static tests

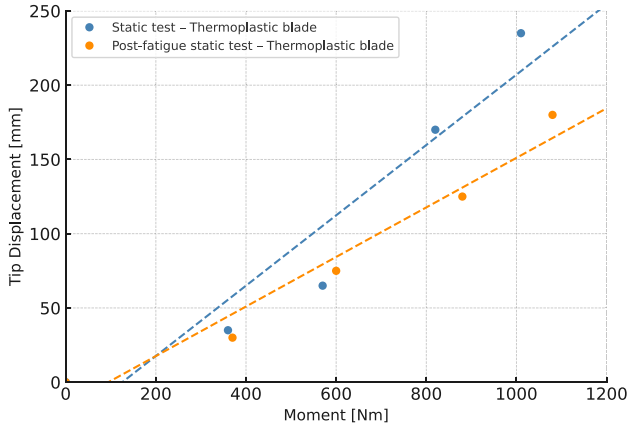

Fig. 13 Tip displacement of thermoplastic blade for initial and final static tests

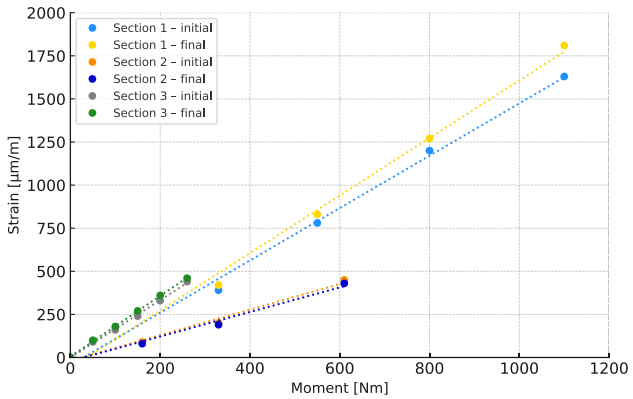

Fig. 14 Strain at different sections of thermoplastic blade for initial and final static tests

means a 23.7%. This deviation of tip displacement at both blades should be reduced increasing the number of a few fiberglass fabrics at the root section during the manufacturing of the blade, to reduce that deviations.

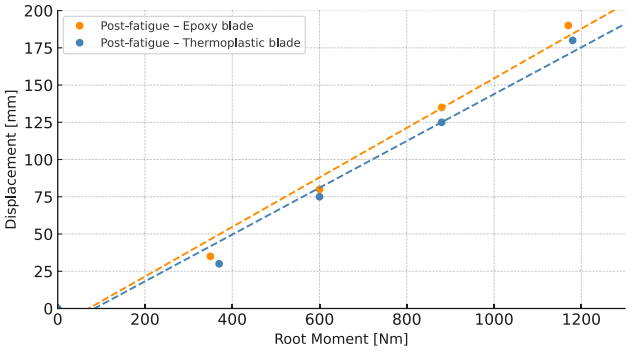

Fig. 15 Measured post-fatigue tip displacement for epoxy and thermoplastic blades under increasing static load

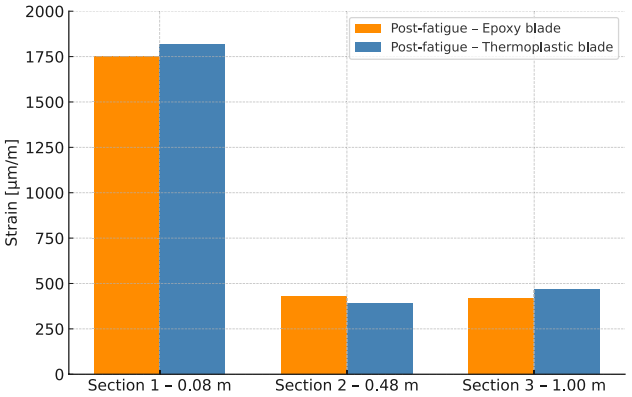

Fig. 16 Measured post-fatigue strain at three blade sections under maximum static load for both blade types

Figure 15 shows the measured blade tip displacement in the flapwise direction as a function of the applied load of the post-fatigue static tests, comparing the epoxy and thermoplastic blade. This was recorded using a string potentiometer positioned at the blade tip. At maximum load, the thermoplastic blade exhibited a tip deflection that was approximately 4.5% lower than that of the epoxy blade. This suggests marginally higher stiffness, possibly due to improved fiber–matrix interaction or more uniform laminate consolidation in the thermoplastic blade. The strain response at three key points along the blade span (0.08 m, 0.48 m, and 1.0 m from the root) was measured using bonded strain gauges. Figure 16 presents the strain values at maximum load of the post-fatigue static test, comparing the epoxy and thermoplastic blade. As expected for a cantilevered beam subjected to distributed bending, both blades exhibited a linear strain gradient along the span. The deviations between the epoxy and thermoplastic blades remained within 10%, confirming that they exhibited similar structural behavior under bending loads.

Following unloading, both blades fully regained their original shape with no visible permanent deformation or delamination. Visual inspection confirmed the absence of matrix cracking, debonding, or fiber wrinkling. This demonstrates that both designs remained within the elastic regime throughout the test and that structural integrity was not compromised. The static test results show that the stiffness and deformation profiles of both the epoxy and thermoplastic blades were comparable under maximum design loads. The thermoplastic blade's slightly lower tip displacement, combined with its consistent strain distribution, confirms its suitability for structural applications in small wind turbine blades.

3.3 Fatigue Response Results

This section presents the results of the fatigue tests conducted on epoxy and thermoplastic blades. These tests aimed to simulate the cumulative damage experienced over a small wind turbine's typical 20–25-year service life by applying 10^6 load cycles under accelerated conditions. As direct load measurement using load cells was not implemented during the test, the applied bending moments were estimated using three strain gauges bonded 0.08 m, 0.48 m, and 1.0 m from the blade root. These strain gauges had been calibrated via static tests prior to the fatigue campaign to ensure accurate strain-to-moment conversion based on known loading conditions.

The fatigue test was designed using the Damage Equivalent Load (DEL) methodology to replicate lifetime damage over a shortened number of cycles. Figure 17 compares the target and applied DEL values for both blades. The close match between target and applied loads verifies the fidelity of the fatigue test protocol and confirms that both blades were subjected to equivalent fatigue demands. Figure 8 shows the initial cyclic response of the epoxy and thermoplastic blade at the three instrumented locations. Both the measured strain and the corresponding bending moments remained stable and within expected ranges. This confirms that the applied loading was evenly distributed and consistent with the designed fatigue profile.

The final test conducted was a property test to compare natural frequencies, center of gravity, and mass. Tables 10 and 11 list the summary of fatigue tests performed to the epoxy and thermoplastic blades respectively. Damage D must be equal or higher than 1 at each section of the blade. Total moment DEL was higher to the target moment at each section for both the epoxy and thermoplastic blades.

Table 10 Summary of fatigue testing results for epoxy blade

Item	Section 1	Section 2	Section 3
Target moment	440	270	120
damage D [-]	1.31	1.05	1.55
DEL [Nm]	452.10	271.21	125.34

Table 11 Summary of fatigue testing results for thermoplastic blade

Item	Section 1	Section 2	Section 3
Target moment	440	270	120
damage D [-]	2.90	4.86	5.12
DEL [Nm]	489.39	316.22	141.30

Figure 17 shows a comparison of the target and applied DELs. This confirms that both blades were subjected to the intended fatigue conditions.

To ensure consistent load application, static calibration tests were performed every 500,000 cycles. In each case, a static load of 150 N was applied 1.44 m from the root, and tip deflection was measured using a string potentiometer. These periodic calibrations helped to track any changes in blade flexibility. Figure 18 shows how blade flexibility, defined as the ratio of tip deflection to applied load, changed throughout the fatigue test. Both the epoxy and thermoplastic blades exhibited less than 2.0% variation in flexibility over 1 million cycles. This indicates negligible structural degradation and confirms that both materials behave elastically under cyclic loading.

After completing 1 million cycles, a detailed inspection was carried out on both blades. No visible damage, delamination, cracking, or loss of stiffness was found on either blade. Minor sensitivity variations of under 2% confirm that the structural integrity of both blade types was maintained throughout the fatigue campaign. The fatigue testing confirmed the durability of the Akelite-based thermoplastic blade, showing performance equivalent to that of the conventional epoxy blade. The structural response remained stable, and no degradation or failure modes were observed,

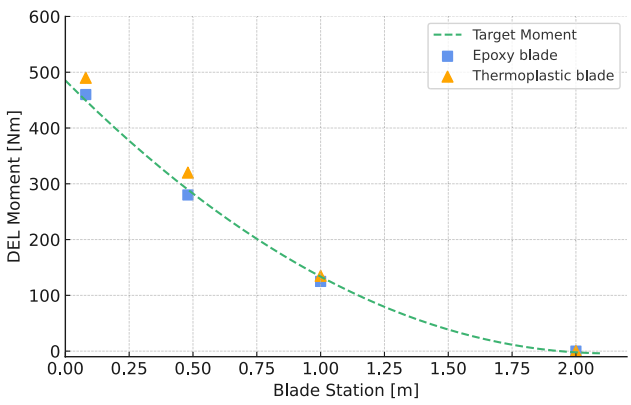

Fig. 17 Target vs. applied damage equivalent loads (DEL) for both blades over 1 million cycles

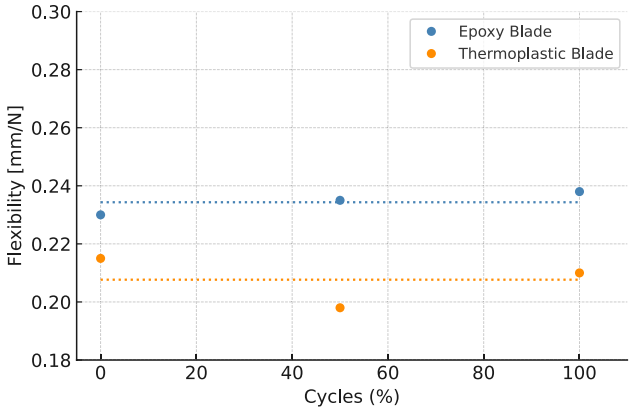

Fig. 18 Flexibility (tip deflection/applied load) of epoxy and thermoplastic blades measured at three calibration points during fatigue testing

Table 12 Mechanical properties of laminates with thermoplastic and epoxy resin [6]

Characteristic	Thermoplastic	Epoxy	Standard
Flexural strength (MPa)	713.4±11.4	724.0±7.4	ASTM D-790
Flexural modulus (GPa)	20.6±1.5	19.9±0.8	ASTM D-790
ILSS (MPa)	41.8±1.7	40.1±2.2	ASTM D-2344

validating the long-term viability of thermoplastic composites in small wind turbine blade applications.

4 Discussion

The certification of new materials, as thermoplastic resin, for wind turbine blades requires its validation on different scales. Table 12 presents the mechanical properties, tensile, bending, and interlaminar strength to the coupon-scale laminates, obtained from previous works and published at [6]. No significant differences were found between both composites, indicating that the thermoplastic resin can be used as polymeric matrix for the manufacturing of fiber reinforced polymer composites.

From blade test results it is possible to estimate the Young's Modulus (E). In our case, using the tip displacement (d) and the applied load during static test, and assuming a value of Inertia moment I=2.25*10⁻7 m^4 at the middle span of the blade, the value of E has been calculated using the following equation:

$$d = \left(\frac{F_1 a_1^2 (3L - a_1)}{6EI}\right) + \left(\frac{F_2 a_2^2 (3L - a_2)}{6EI}\right), \quad (4)$$

where

– d is the tip displacement obtained from static test [m],
– F_1=F_2=500 N is the applied loads,
– a_1=0.64 m and a_2=1.44 m are the load sections,
– L is the blade length L=2 m,
– E is the Young's Modulus [GPa],
– I is the Inertia moment [m^4].

For the epoxy blade, the tip displacement during static test was d=15.3 cm, so the modulus of elasticity obtained using the previous equation was E=28.22 GPa. In the case of the thermoplastic blade, and with a tip displacement of d=23.4 cm obtained during static blade, the value of the modulus of elasticity was E=18.45 GPa. These values obtained from the elasticity modulus for the two blades (with epoxy resin and with thermoplastic resin) are reasonable for a GFRP composite material, considering that the fibers are not 100% oriented in the longitudinal direction, having also included fibers at 45° and 90°. Epoxy blade is more rigid than the thermoplastic one.

An experimental comparison was conducted between two wind turbine blades, each 2 ms long, with identical geometry and fiber architecture. One blade was manufactured using a thermoset epoxy resin, while the other used the novel Akelite thermoplastic resin. The evaluation included characterizing the properties, conducting static mechanical testing and assessing fatigue performance. Finally, a post-fatigue static test and a final property test were performed to evaluate the behavior of the blades. Using a single mold and the same VARI process ensured consistent conditions for both blade types. Substituting the resin matrix was the only variable, enabling a direct comparison of structural performance. The thermoplastic blade had a mass that was 7.3% lower and a center of gravity that was closer to the root. These differences are favorable, particularly in distributed wind systems, where lighter components simplify transport and installation.

Post-fatigue static testing revealed minimal differences between the blades. The thermoplastic blade exhibited a 4.5% lower tip deflection under peak design load (1,140 Nm), and the strain profiles showed deviations of less than 10%. These results suggest that Akelite-based laminates have flexural stiffness and load response properties that are at least equivalent to those of conventional epoxy systems. The absence of permanent deformation confirms that both blades remained within the elastic regime, thus validating their design under extreme static conditions. The fatigue campaign consisted of 10^6 load cycles and simulated long-term operational stress. Monitoring strain and flexibility during the test showed variations of less than 2%, demonstrating negligible degradation in structural stiffness. Post-test inspections revealed no visible damage, such as cracking, delamination, or matrix failure. These results confirm that the thermoplastic resin offers excellent fatigue resistance,

in line with recent studies on acrylic-based thermoplastics [9, 12].

The use of thermoplastic composites in wind turbine blades presents several advantages. Beyond structural parity, they offer:

- improved recyclability through remelting or solvent dissolution;
- shorter curing cycles and reduced energy consumption during manufacturing;
- fusion bonding capability for repair and modular blade design.

The recycling process developed for this thermoplastic blade was similar to described at [7], with a dissolution of the blade in a solvent. In that case, acetone was used as a solvent and the study of recyclability of a small thermoplastic blade was carried out with percentages of resin and fibers recovered more than 80%. These quantities of recovered resin and fibers were reused to manufacture a new blade shells with the recovered materials during the recycling process.

The current cost of Akelite resin is slightly higher than that of commercial epoxy resins, extrapolations for industrial-scale manufacturing suggest that the difference would be negligible due to economies of scale and reduced energy requirements in the production process. In view of these benefits, Akelite resin seems to be a promising candidate for small wind blade applications that prioritize sustainability and reducing lifecycle costs.

5 Conclusions

This study compared the structural performance of two wind turbine blades with identical geometry and fiber architecture, the only difference being the matrix material: standard epoxy resin or the novel thermoplastic resin Akelite.

- The thermoplastic blade exhibited a 7.3% lower mass and a 13.3% higher flapwise natural frequency compared to the epoxy blade.
- Under static loading, both blades showed similar strain profiles and stiffness. The thermoplastic blade deflected 4.5% less than the epoxy blade.
- Fatigue testing over 1 million cycles revealed less than 2% variation in flexibility and no observable structural degradation.

Both blades passed all structural tests without sustaining any damage. These results demonstrate that thermoplastic resins, specifically Akelite, can effectively replace epoxy resin in the manufacture of small-scale wind turbine blades, offering environmental and economic advantages. A deviation of tip displacement at both blades close to 20% should be reduced increasing the number of fiberglass fabrics at the root section during the manufacturing of the blades. In addition, manual manufacturing (bonding of two valves) could be affect to this deviation. Future work will focus on scaling up the process for larger blade lengths (e.g., 11 ms), incorporating accelerated aging tests, and validating recyclability through post-use thermomechanical reprocessing. The aim of these efforts is to establish thermoplastic composites as a sustainable alternative in distributed wind energy systems.

Acknowledgements This research was funded by the AEI Agency of the Ministry of Science, Innovation and Universities of the Spanish Government, under Grant No. TED2021-130201B-C33, by NextGenerationEU European Funds, and PID2023-151110OB-I00.

Funding Open Access funding provided thanks to the CRUE-CSIC agreement with Springer Nature.

Data Availability The data from this work are available upon request from the authors.

Declarations

Conflict of interest The authors declare no conflict of interest.

References

1. J. Jensen, K. Skelton, Wind turbine blade recycling: experiences, challenges and possibilities in a circular economy. Renew. Sustain. Energy Rev. **97**, 165–176 (2018). https://doi.org/10.1016/j.rser.2018.08.041
2. M.J. Leon, Recycling of wind turbine blades: recent developments. Curr. Opin. Green Sustain. Chem. **39**, 100746 (2023). https://doi.org/10.1016/j.cogsc.2022.100746
3. L. Mishnaevsky, Sustainable end-of-life management of wind turbine blades: overview of current and coming solutions. Materials (2021). https://doi.org/10.3390/ma14051124
4. Iec 61400-23: 2014 – wind turbines – part 23: Full-scale structural testing of rotor blades. International Electrotechnical Commission (2014). Standard IEC 61400-2:2013
5. LM Wind Power. Zebra project launched: toward 100% recyclable wind turbine blades. https://www.lmwindpower.com/en/stories-and-press/stories/news-from-lm-places/zebra-project-launched (2023). Accessed 24 April 2025
6. R. Carnicero, L. Cano, M.A. Lopez-Manchado, R. Verdejo, Manufacturing, testing and recycling of a small recyclable wind turbine

blade. J. Phys: Conf. Ser. **2265**(3), 032013 (2022). https://doi.org/10.1088/1742-6596/2265/3/032013
7. R. Carnicero, L. Cano, I. Cruz, Lessons learned from the sustainable recycling process of a wind blade made with a new thermoplastic resin. J. Phys. Conf. Ser. **2767**(7), 072008 (2024). https://doi.org/10.1088/1742-6596/2767/7/072008
8. J. Garate, S.A. Solovitz, D. Kim, Fabrication and performance of segmented thermoplastic composite wind turbine blades. Int. J. Precis. Eng. Manuf. Green Technol. **5**(2), 271–277 (2018). https://doi.org/10.1007/s40684-018-0028-3
9. E. Boissin, C. Bois, J.C. Wahl, T. Palin-Luc, D. Caous, Ply scale modelling of the quasi-static and fatigue behaviours of an acrylic-thermoplastic-matrix and glass-fibre-reinforced laminated composite covering the service temperature range of wind turbine blades. Int. J. Fatigue **152**, 106413 (2021). https://doi.org/10.1016/j.ijfatigue.2021.106413
10. T.H.L. Pinto, W. Gul, L.A.G. Torres, C.A. Cimini, S.K. Ha, Experimental and numerical comparison of impact behavior between thermoplastic and thermoset composite for wind turbine blades. Materials **14**(21), 6377 (2021). https://doi.org/10.3390/ma14216377
11. Z. Arwood, D.S. Cousins, S. Young, A.P. Stebner, D. Penumadu, Infusible thermoplastic composites for wind turbine blade manufacturing: static characterization of thermoplastic laminates under ambient conditions. Compos. Part C Open Access **11**, 100365 (2023). https://doi.org/10.1016/j.jcomc.2023.100365
12. D.S. Cousins, Z. Arwood, S. Young, B. Hinkle, D. Snowberg, D. Penumadu, A.P. Stebner, Infusible thermoplastic composites for wind turbine blade manufacturing: fatigue life of thermoplastic laminates under ambient and low-temperature conditions. Adv. Eng. Mater. (2023). https://doi.org/10.1002/adem.202201941
13. R.E. Murray, D. Penumadu, D. Cousins, R. Beach, D. Snowberg, D. Berry, Y. Suzuki, A. Stebner, Manufacturing and flexural characterization of infusion-reacted thermoplastic wind turbine blade subcomponents. Appl. Compos. Mater. **26**(3), 945–961 (2019). https://doi.org/10.1007/s10443-019-9760-2
14. R. Verdejo, M. López-Manchado. Fiber reinforced polymers based on thermoplastic matrices. Granted patent. (2021)
15. Ictp. URL https://www.ictp.csic.es/index.php/es
16. K. Van Rijswijk, et al., Thermoplastic composite wind turbine blades. Technical University Of Delft (2007)
17. L.C. Forcier, S. Joncas, Development of a structural optimization strategy for the design of next generation large thermoplastic wind turbine blades. Struct. Multidiscip. Optim. **45**, 889–906 (2012)
18. D.S. Cousins, *Advanced thermoplastic composites for wind turbine blade manufacturing* (Colorado School of Mines, 2018)
19. X. Cheng, B. Du, J. He, W. Long, G. Su, J. Liu, Z. Fan, L. Chen, A review of thermoplastic composites on wind turbine blades. Compos. Part B **11**, 112411 (2025)
20. C. Hao, B. Zhao, X. Guo, S. Zhang, M. Fei, L. Shao, W. Liu, Y. Cao, T. Liu, J. Zhang, Mild chemical recycling of waste wind turbine blade for direct reuse in production of thermoplastic composites with enhanced performance. Resour. Conserv. Recycl. **215**, 108159 (2025)
21. M. Zivkovic, Manufacturing of a fiber-reinforced thermoplastic composite micro-generating wind turbine blade. MASc Thesis, University of Waterloo (2023)
22. R.E. Murray, R. Beach, D. Barnes, D. Snowberg, D. Berry, S. Rooney, M. Jenks, B. Gage, T. Boro, S. Wallen, S. Hughes, Structural validation of a thermoplastic composite wind turbine blade with comparison to a thermoset composite blade. Renew. Energy **164**, 1100–1107 (2021). https://doi.org/10.1016/j.renene.2020.10.040
23. L.M. Jr., How to repair the next generation of wind turbine blades. Energies (2023)
24. M.J. Leon, Recycling of wind turbine blades: recent developments. Curr. Opin. Green Sustain. Chem. **39**, 100746 (2023). https://doi.org/10.1016/j.cogsc.2022.100746
25. D. Marten, Qblade: a modern tool for the aeroelastic simulation of wind turbines. Ph.D. thesis (2020). https://doi.org/10.14279/depositonce-10646. URL https://depositonce.tu-berlin.de/bitstream/11303/11758/4/marten_david.pdf
26. D. Systèmes, Solidworks https://www.solidworks.com/
27. M. Desmond. Bladefs software. National Renewable Energy Laboratory (NREL) (2010). https://www.nrel.gov/wind/nwtc/bladefs.html
28. M.S. Selig, P. Giguère, Effects of thickness and camber on airfoil performance. Tech. Rep. UILU-ENG-95-0181, University of Illinois at Urbana-Champaign (1995). URL https://m-selig.ae.illinois.edu/pubs/Selig-1995-AFOSR-TR-95-3030.pdf. Report No. AFOSR-TR-95-3030
29. Gavazzi Tessuti Tecnici. Technical fabrics for composite applications. https://www.gavazzispa.it/ (2025). Accessed 15 May 2025
30. Sicomin Epoxy Systems. Epoxy resins and composite materials. https://www.sicomin.com (2025). Accessed 15 May 2025
31. CATEC. Discovery 3d printer – large format industrial additive manufacturing. https://discovery3dprinter.com/es/discovery-3d-printer/ (2025). Accessed 15 May 2025
32. SABIC. Lnp™ thermocomp™ ac004xxar1: Carbon fiber reinforced abs. https://www.sabic.com (2025). Accessed 15 May 2025
33. Sicomin Epoxy Systems. Isobond 735 – two-component epoxy structural adhesive. https://www.sicomin.com/structural-adhesives/isobond-735 (2025). Accessed 15 May 2025
34. Iec 61400-2:2013 – wind turbines – part 2: Small wind turbines. International Electrotechnical Commission. Standard IEC 61400-2:2013 (2013)
35. D. Wood, *Small Wind Turbines: analysis, design, and application* (2011). URL https://www.amazon.com/Small-Wind-Turbines-Application-Technology/dp/1849961743